J Electr Eng Technol Vol. 9, No. 4: 1315-1323, 2014
http://dx.doi.org/10.5370/JEET.2014.9.4.1315

ISSN(Print) 1975-0102
ISSN(Online) 2093-7423

# Optimum Rotor Shaping for Torque Improvement of Double Stator Switched Reluctance Motor

**Mohammadali Tavakkoli† and Mehdi Moallem***

**Abstract** - Although the power density in Double Stator Switched Reluctance Motor (DSSRM) has been improved, the torque ripple is still very high. So, it is important to reduce the torque ripple for specific applications such as Electric Vehicles (EVs). In This paper, an effective rotor shaping optimization technique for torque ripple reduction of DSSRM is presented. This method leads to the lower torque pulsation without significant reduction in the average torque. The method is based on shape optimization of the rotor using Finite Element Method and Taguchi's optimization method for rotor reshaping for redistribution of the flux so that the phase inductance profile has smoother variation as the rotor poles move into alignment with excited stator poles. To check on new design robustness, mechanical analysis was used to evaluate structural conformity against local electromagnetic forces which cause vibration and deformation. The results show that this shape optimization technique has profound effect on the torque ripple reduction.

**Keywords**: Double stator switched reluctance motor, Finite element method, Mechanical stress analysis, Torque ripple reduction

## 1. Introduction

Switched Reluctance Motors (SRM) has unique capabilities of operation in super high speeds and harsh environment. So, they are good candidates for industrial and automotive applications. Because of absence of the excitation winding on the rotor, they are not susceptible to rotor winding faults and demagnetization or flying off the magnets. Also, owing to its stiff structure and the absence of the magnetic source on the rotor, an SRM is inherently robust and cheap.

In spite of its advantages, SRM has a nonlinear and complex behavior due to local saturation of some rotor and stator iron parts and doubly salient structure. This affects the overall performance of the motor. Two of the SRM disadvantages are high torque ripple and low power density as compared to PMS motors. Switched-reluctance motors produce acoustic noise and vibration caused by torque ripple and normal forces acting on the rotor and stator surfaces. Application of these motors where silent operation is desirable, such as in home appliances, has, thus, been limited. Therefore, a large improvement in power density and torque ripple is necessary for SRM before it can be chosen as suitable candidate for such applications. The improvement in power density was made possible by new design of double stator switched reluctance motor which was introduced in [1]. However, the problem of high torque ripple is remained unsolved in this motor too.

Over the last two decades different advanced control and design strategies have been developed for torque ripple reduction, but due to high torque pulsation especially at low speeds those controls and design strategies has not been effective to reach the acceptable torque characteristics. In [2] a new technique of generating optimal current commands for SRM drives is presented. Authors have used a small set of Fourier coefficients rather than a large set of discrete points. Reference [3] presents a torque ripple minimization controller realized by indirect position and speed sensing for switched reluctance motors (SRMs). A method of torque ripple reduction for low speed SRM drives has been presented in [4]. The method includes a new PWM current control strategy where the current follows a contour for constant torque production.

A new current shape required for a low torque ripple switched reluctance motor for high speed applications is introduced in [5]. An early attempt to minimize torque ripple using Torque Sharing Functions (TSFs) is presented by Illic-Spong et al. in [6]. This method uses exponentially rising and decreasing TSFs. A method which minimizes the peak current requirements of the phase while requires linear change in the rotor angular variation during phase commutation is investigated in [7]. An advanced control system that uses the linear motor and load model and decouples the control requirements of the SRM phases originated from the work of Taylor et al. [8, 9]. Author in [10] presents a review on previous methods used to mitigate torque ripple in SRM drives. Authors in [11] presented a genetic algorithm for switched reluctance motor design optimization. They used a novel multi-

† Corresponding Author: Dept. of Electrical and Computer Engineering, Isfahan University of Technology, Iran. (mtavakkoli2002@yahoo.com)
* Dept. of Electrical and Computer Engineering, Isfahan University of Technology, Iran. (moallem@cc.iut.ac.ir)
Received: October 29, 2013; Accepted: February 14, 2014

objective optimization method based on a Genetic-Fuzzy Algorithm (GFA) for torque ripple mitigation. In [12], to reduce the torque pulsation, a novel SRM appropriate for use in hybrid electric vehicles with more rotor poles than stator poles is represented. This paper claims that a 6/10 SRM produces a higher average torque and lower torque pulsation compared with a 6/4 SRM. Reference [13] introduces a new and efficient commutation algorithm for torque ripple reduction. The commutation algorithm is speed dependent and uses a real time approach instead of pre-calculated stored data. In [14], a new rotor shape design is presented to mitigate the torque ripple of switched reluctance motor. Authors in [15] describe a proposal for a new stator pole face having a non-uniform air-gap and a pole shoe attached to the lateral face of the rotor pole. These additions minimize the undesired torque ripple. The effects of each design parameter are investigated using a time-stepping finite-element method. Authors in [16] use additional teeth per rotor and stator pole to mitigate the torque ripple. Reference [17] briefly describes an approach to determine the optimum magnetic circuit parameters to minimize low speed torque ripple for switched reluctance (SR) motors. In [18] an electromagnetic analysis of the switched-reluctance (SR) machine with saw-shaped (shark) pole surfaces was presented. This design aspect facilitates an increase of the 'maximum/minimum' inductance ratio, relative to the flat-pole structure. Authors in [19] investigated the effect of the rotor profile on the produced torque of SRM. Authors in [20] present a numerical multi-objective optimization procedure by using finite element simulation, the Kringing model and Pareto archived evolution strategy. Reference [21] introduces a new and efficient commutation algorithm for torque ripple reduction. The commutation algorithm is speed dependent and uses a real time approach instead of pre-calculated stored data. Authors in [22] present the design and operation of a two-phase four-two pole SRM for a high-speed air blower. In [23] a novel method of eliminating the torque ripple in the instantaneous torque profile of SRM is presented, and a method to generate the precise reference phase current waveforms for even open loop operational design through global optimization is investigated.

Before invention of double stator switched reluctance motor (DSSRM) [1], as shown in Fig. 1, power density of the switched reluctance motor was not comparable with that of PM motors. So, PM motors are more popular than switched reluctance motors in many applications. In conventional SRM, force components are used inappropriately, therefore, the developed torque was lower than motor real capability. To overcome that deficiency, larger normal force components in DSSRM are used to produce a higher average torque. In the switched reluctance motor, the normal force density is much larger than the tangential force density, whereas the normal force is troublesome and the tangential force is used for torque production. It was necessary to design a new structure which uses the larger

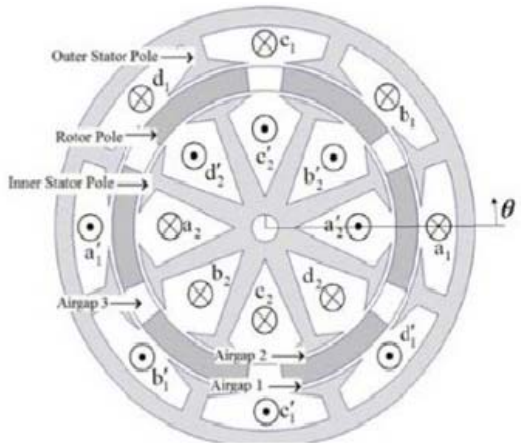


**Fig. 1.** Cross section of 4- phase DSSRM

part of the produced force to move the rotor. In DSSRM, the motion direction is aligned to flux path (as shown in Fig. 2) and the larger force component is moving the rotor. The most important advantage of DSSRM is its high power density, and its adverse characteristic is the high torque pulsation in domestic and automotive applications where the high torque pulsation is not acceptable.

In this paper, we try to reduce the torque ripple of DSSRM by modification in force components which depends on the profile of stator phase inductance. Our preliminary analysis resulted in an initial rotor shape. However, due to mechanical and manufacturing constraints, initial shape is substituted by 4 holes in the rotor poles. Next, we optimized the holes radii and positions by using the Taguchi's optimization Method. The outline of the rest of this paper is as follows; section II presents a brief description of the DSSRM construction and model. Section III explains the optimization process. Section IV presents the results of torque ripple for new design, and Section V investigates the mechanical conformity of the new rotor shape against vibration and deformation.

## 2. DSSRM Description

Energy Conversion Efficiency in SRM is defined in [1] as follows:

$$ECE(\theta,i)=\frac{F_{motional}(\theta,i)}{F_{motional}(\theta,i)+F_{non-motional}(\theta,i)}*100 \qquad (1)$$

Where, $F_{motional}$ , is the net force generated in the direction of motion, and $F_{non-motional}$ is the total force perpendicular to the motion direction. In this machine, two stators are used. These stators are made of laminated ferromagnetic material (M-19) and are equipped with concentrated windings. The two stators are located on the interior and exterior of a cylindrical rotor. The rotor is formed by segments of laminated M-19, which is hold

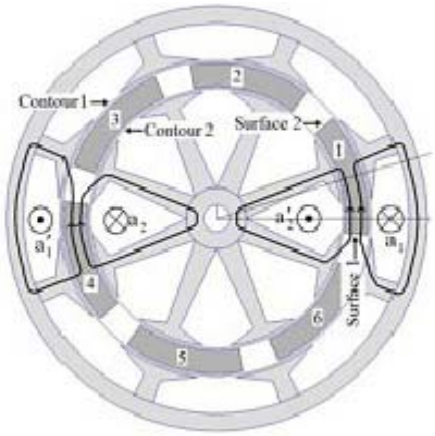


**Fig. 2.** DSSRM flux lines whit phase 'a' excited to move the rotor clockwise

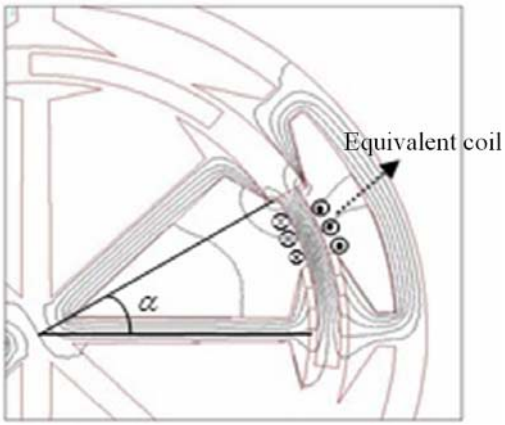


**Fig. 3**. Flux lines of one equivalent coil

together using a non-ferromagnetic cage. In the proposed DSSRM, the number of stator and rotor poles (segments) is 8 and 6, respectively. DSSRM is a reluctance motor with higher ECE compared to ordinary Switched Reluctance Motor. Reluctance variation is the main cause of the developed torque in SR motors; therefore, it is important to improve phase inductance profile to improve its performance. Looking at flux path in DSSRM as shown in Fig. 2, it can be realized that two sides of the inner and outer stator phase windings such as ($a_1$, $a_2'$) and ($a_1'$, $a_2$) can be assumed as the separate windings, which simplify the analysis (Fig. 3). The electrical model of DSSRM includes one resistance which models the equivalent coil resistance and one variable inductance modeling the equivalent coil inductance. Because one side of the equivalent coil involves the outer stator phase and the other side involves the inner stator phase, the equivalent coil inductance is almost identical with each stator phase winding and its resistance is the average of outer and inner stator phase windings (Fig. 4). In this model, determination of the accurate inductance of equivalent coil is important.

Nonlinear relationship between the flux linkages and the currents has made it much more difficult to analytically

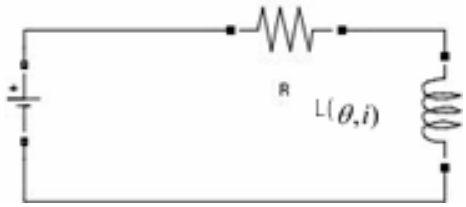


**Fig. 4.** Schematic of equivalent circuit of DSSRM

represent the phase inductance or the flux linkages as a function of current and position for the entire ranges of operation. Therefore, the calculation of related machine variables are typically performed using a numerical analysis method, such as Finite Element (FE) method. In this paper, to compare the conventional SRM with the proposed DSSRM, a FE analysis considering magnetic saturation has been carried out. FEM is a powerful tool to calculate the inductance of the equivalent coil at different positions and different currents. This will result in a look up table for equivalent coil inductance. Since the rotor is a part of the magnetic flux path, the motion and saturation of the rotor in some positions changes the flux path reluctance and causes the change in the equivalent coil inductance. So, inductance is a function of the rotor position and the stators currents.

According to Fig. 4, the circuit equations of DSSRM canbe written as:

$$V = Ri(t) + \frac{\partial \lambda(i,\theta)}{\partial t} \tag{2}$$

$$\frac{\partial \lambda(i,\theta)}{\partial t} = \frac{\partial \lambda}{\partial i}\frac{\partial i}{\partial t} + \frac{\partial \lambda}{\partial \theta}\frac{\partial \theta}{\partial t} \tag{3}$$

$$\frac{\partial \lambda}{\partial i} = L_{inc}\ ,\ \frac{\partial \lambda}{\partial \theta} = L_w \tag{4}$$

Summarizing (2), (3) and (4)

$$\frac{\partial i}{\partial t} = \frac{V - Ri - \omega L_w}{L_{inc}} \tag{5}$$

The torque equations in linear region of inductance are

$$W(i,\theta) = \frac{1}{2}L(\theta)i^2 \tag{6}$$

$$T = \frac{\partial Wc(i,\theta)}{\partial \theta} = \frac{1}{2}i^2\frac{\partial L(\theta)}{\partial \theta} \tag{7}$$

Where V is the input voltage, R is the equivalent coil resistance, i(t) is the equivalent coil current, is the flux linkage, $\omega$ is the mechanical angular velocity and *Wc* is the magnetic energy. As it can be seen from equation (6), the smooth torque profile depends on the slope of L(θ) and constant results in the constant torque. Since $\frac{\partial L(\theta)}{\partial \theta}$ is a result of the rotor position, rotor pole shaping is the best

option to smooth the inductance slope and suppress the torque pulsation.

## 3. Rotor Shaping and Optimization Process

To smooth the torque profile, it is necessary to change the inductance profile gradually as the rotor pole moves into alignment with the excited stator poles. The proposed shape must be analyzed in accordance with the present motor structure because the stator windings are already designed and the rotor must be examined in the existing structure. Fig. 2 shows clearly that the flux paths of the two stators windings are independent; so, any change in the rotor structure must be performed for each of two flux paths. To reduce the rate of the inductance change, it is necessary to increase the flux path reluctance as the rotor moves. One way to increase the reluctance of the flux path is to increase the saturation at the tip of the rotor poles. The maximum rate of inductance change happens when the alignment between the rotor and stator poles begins. So, in this position the rotor reluctance should be increased to cause the smoother inductance change. To do so, the rotor may be cut as shown in Fig. 5. The proposed rotor shape in Fig. 5 causes the saturation in the rotor pole tips close to the edges as shown in Fig. 6. Fig. 7 shows the smoothness obtained in phase inductance caused by this new shape.

Manufacturing the rotor shape of the Fig. 5 is difficult and operation of rotor will this rotor shape will make noise and vibration problems; so, we propose to use four circular holes to shape the rotor poles close to the shape in the Fig.

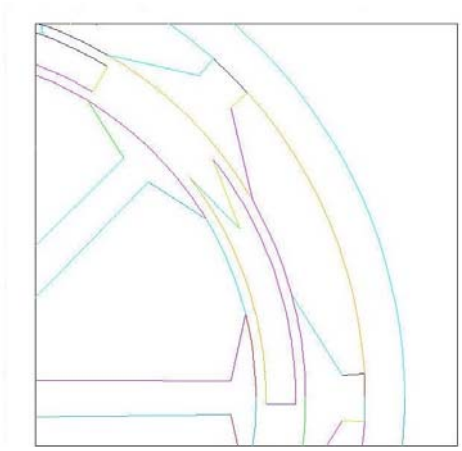

**Fig. 5.** Suggested preliminary rotor pole shape for DSSRM

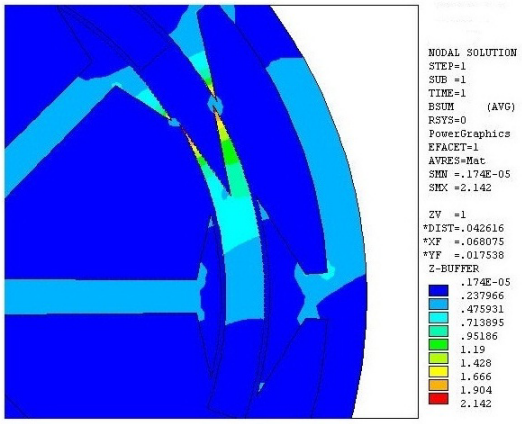


**Fig. 6.** Magnetic flux density in the rotor structure after rotor shaping

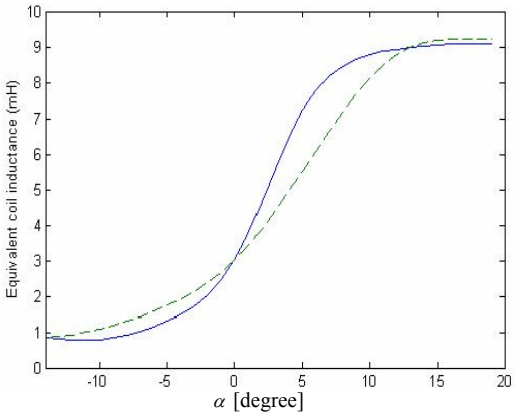


**Fig. 7.** Equivalent coil inductance before (--) and after (-) rotor shaping

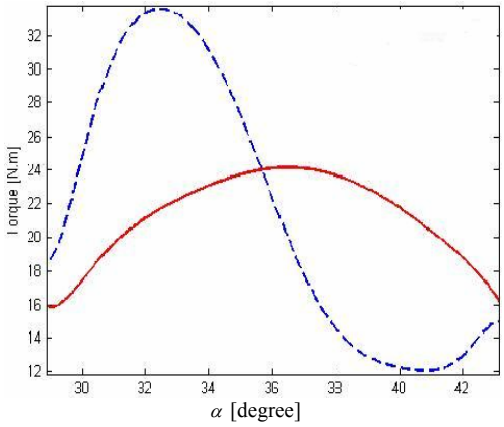


**Fig. 8.** Static torque before (--) and after (-) rotor pole shaping

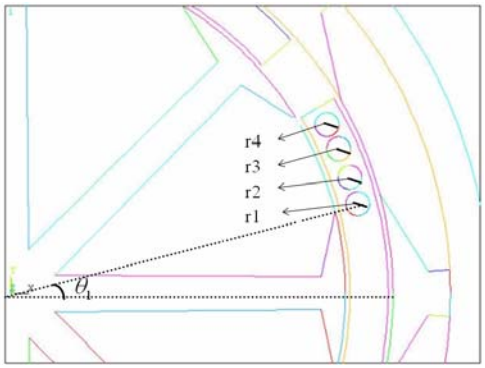


**Fig. 9.** Use of the circular holes for practical rotor shaping

5 which is shown in Fig. 9.

In Fig. 9, ri is the radius of ith circle and $\theta$ i is the angle between center of circle i and the horizontal dashed line.

Torque ripple is defined as:

$$T_{ropple} = \frac{T_{\max} - T_{\min}}{T_{av}} * 100 \quad (8)$$

The average Torque of DSSRM before changing the rotor structure is 21.26 Nm, the maximum and minimum torques are 33.8 Nm and 12.2 Nm respectively. According to equation (7), torque ripple before changing the rotor structure is 101.6%. In the next step, we use Taguchi's method to optimize the holes attributes for minimum torque ripple.

Orthogonal Arrays (OAs) which have a profound background in statistics [24, 25], play an essential role in Taguchi's method. Orthogonal arrays were introduced in the 1940s and have been widely used in designing of the experiments since then. They provide an efficient and systematic way to determine control parameters so that the optimal result can be found with only a few experimental runs. Taguchi's method uses orthogonal arrays to design experiments according to number of optimization parameters and parameters levels. Taguchi's experiments designs are presented under the name 'Taguchi's Tables'. Therefore, using Taguchi's method is extremely easy and efficient. Taguchi's Method has several stages as follows:

### 3.1 Problem initialization

The optimization procedure starts with the problem initialization, which includes the selection of a proper OA's and suitable objective function. The selection of an OA mainly depends on the number of input parameters and their levels. Initial parameters levels are selected based on the user experience or the maximum and minimum of the optimization range as follows:

$$LD = \frac{\max - \min}{number\ of\ levels + 1} \quad (9)$$

Where, *LD* is called the level difference.

### 3.2 Conduct experiments

After determining the input parameters and objective function, each experiment can be calculated and the obtained results are used for analysis based on the user requirements.

### 3.3 Identify optimal level values

Using definition for an objective function it is possible to determine the best design parameters according to the experimental results.

In Fig. 10 all steps in Taguchi's method are presented briefly.

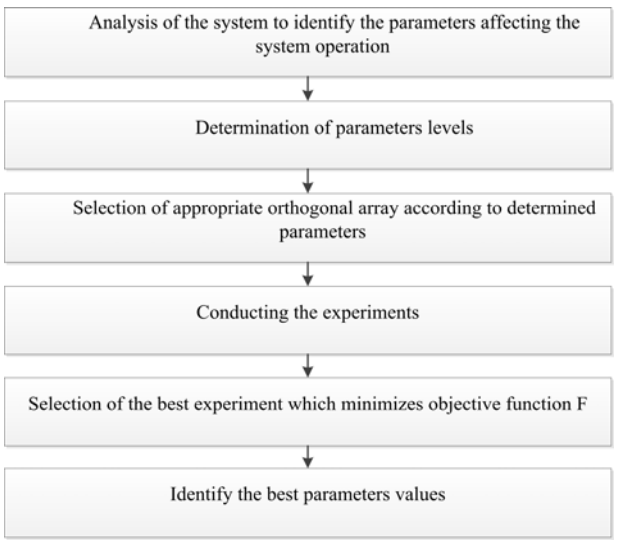


**Fig. 10.** A simple flowchart of Taguchi's Method

## 4. Results and Discussion

Selected parameters and levels are given in Table 1. They were selected such that the rotor structure is closely similar to the rotor structure in Fig. 5. Defining an objective function, it is possible to determine the best design parameters. Our objective function is:

$$F = \left(\frac{T_{av}}{T_{\max} - T_{\min}}\right) p \quad (10)$$

$$p(\ penalty\ \ factor) = \begin{cases} 0 & T_{av} < 20.62 \\ 1 & T_{av} \geq 20.62 \end{cases} \quad (11)$$

In our optimization process, the maximum permissible average torque decrease is chosen as 3% that is why the 20.62Nm is selected as the critical value for changing the penalty factor (p).

The best design provides the maximum value of the function F. For F values given in Table 2, the best design parameters are obtained at row 14 and the parameters levels in experiment 14 are shown in Table 3. The

**Table 1.** Eight variables and their different levels

| Variable | Level 1 | Level 2 | Level 3 |
|---|---|---|---|
| r1 | 1.2(mm) | .8(mm) | |
| r2 | 1.6(mm) | 1.2(mm) | 0.8(mm) |
| r3 | 2.1(mm) | 1.8(mm) | 1.5(mm) |
| r4 | 3.3(mm) | 3.2(mm) | 3.1(mm) |
| θ1 | 0.255(rad) | 0.253(rad) | 0.25(rad) |
| θ2 | 0.315(rad) | 0.31(rad) | 0.305(rad) |
| θ3 | 0.395(rad) | 0.39(rad) | 0.385(rad) |
| θ4 | 0.49(rad) | 0.485(rad) | 0.48(rad) |

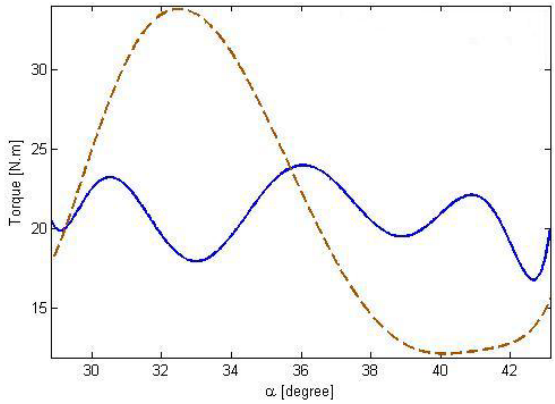


**Fig. 11.** Static torque before (--) and after (-) optimization

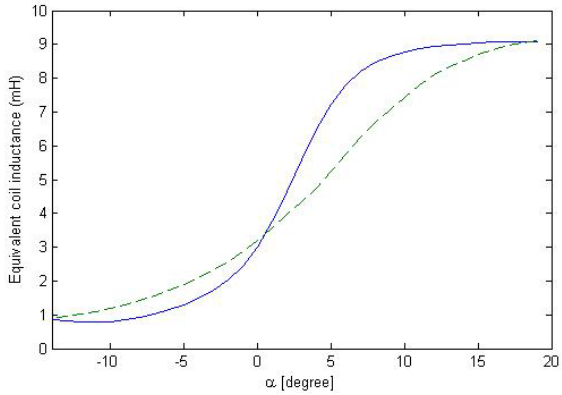


**Fig. 12.** Equivalent coil inductance before (--) and after (-) optimization

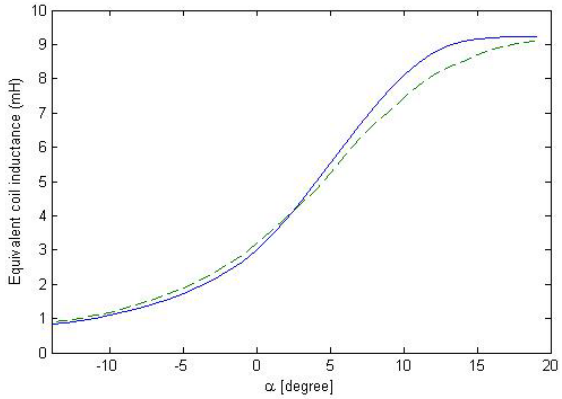


**Fig. 13.** Equivalent coil inductance after saw shaping of the rotor (-) and after optimization (--)

produced torque of DSSRM before and after rotor pole shaping and the equivalent coil inductance are shown in Figs. 11 and 12 respectively. As shown in Fig. 11, the new proposed rotor shape has a noticeable effect in smoothing the static torque.

Taguchi's experiments results are shown in Table 2.

Fig. 13 shows that the rotor shape after optimization improves the inductance profile more than the saw shaping.

**Table 2.** The results of Taguchi's method

| Experiment | Average torque [N.m] | Torque ripple [%] | F |
|---|---|---|---|
| 1 | 20.58 | 42.9 | 0 |
| 2 | 20.63 | 47.6 | 2.1 |
| 3 | 20.66 | 56.1 | 1.78 |
| 4 | 20.6 | 51.2 | 0 |
| 5 | 20.61 | 65.5 | 0 |
| 6 | 20.62 | 32.1 | 3.11 |
| 7 | 20.42 | 44.3 | 0 |
| 8 | 20.61 | 55.46 | 0 |
| 9 | 20.58 | 68.96 | 0 |
| 10 | 23.04 | 105.2 | 0 |
| 11 | 20.8 | 37.15 | 2.69 |
| 12 | 21 | 54.5 | 1.83 |
| 13 | 20.77 | 66.77 | 1.5 |
| 14 | 20.76 | 30.7 | 3.26 |
| 15 | 20.87 | 36.5 | 2.74 |
| 16 | 20.7 | 51.7 | 1.93 |
| 17 | 20.84 | 62 | 1.61 |
| 18 | 20.6 | 29.5 | 0 |

**Table 3.** Optimal parameters

| Parameter | Optimized value |
|---|---|
| r1 | 0.8mm |
| r2 | 1.2mm |
| r3 | 2.1mm |
| r4 | 3.3mm |
| $\theta_1$ | 0.253rad |
| $\theta_2$ | 0.305rad |
| $\theta_3$ | 0.39rad |
| $\theta_4$ | 0.48rad |

**Table 4.** Torque characteristics of DSSRM before and after optimization

| | Before optimization | After optimization |
|---|---|---|
| Average Torque (N.m) | 21.26 | 20.76 |
| Torque Ripple% | 101.6 | 30.7 |

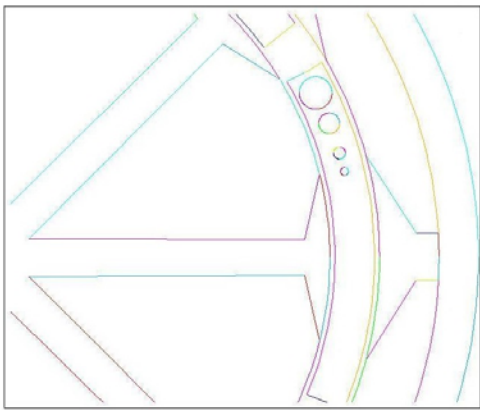

**Fig. 14.** Optimal rotor shape design

As it can be seen in row 14 of Table 2, the minimum torque ripple is 30.7% at average torque of 20.76 Nm.

The optimum rotor shape and optimum parameters

valuesare shown in Fig. 14 and Table 3 respectively. In Table 4 torque characteristics before and after optimization are compared.

Table 4 shows clearly the effectiveness of the proposed rotor structure.

## 5. Mechanical Analysis

In this section, the proposed rotor shape including 4 holes in the rotor structure is analyzed mechanically to check for the rotor conformity. One of the most critical parts of the rotor is the wall between two larger holes. To evaluate the conformity of the rotor structure a 3D Finite Element analysis was used. In the first step the electro-magnetic equations were solved using 3D FEM to obtain the local forces affecting the rotor structure. Then, mechanical equations involving the local electromagnetic forces from step 1 were solved using 3D FEM in speed of 1500 rpm. The maximum stress in the rotor structure and the rotor deformation for one position are shown in Figs. 15 and 16 respectively. As it can be seen, the maximum stress of the rotor structure is much less than the critical deforming stresses (the mechanical stress in which deformation starts is 49 GPa) for the optimized rotor shapes. So, the proposed rotor structure can be used for suppression of torque pulsation.

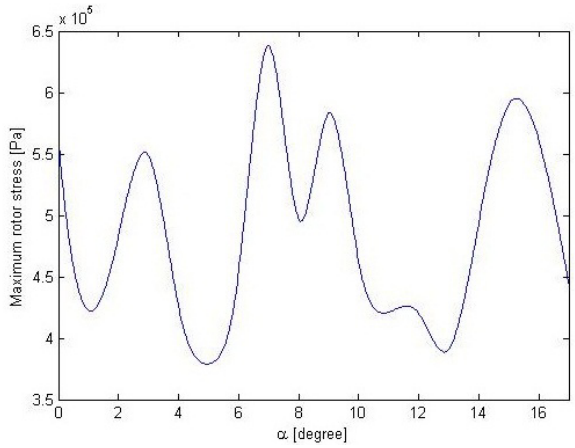


**Fig. 15.** Maximum rotor mechanical stress

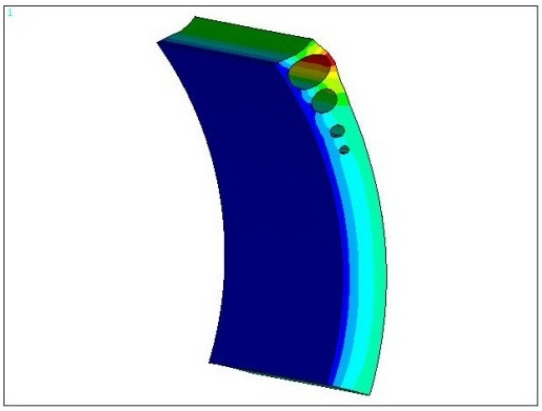

**Fig. 16.** Rotor deformation (Scaled by 30000)

## 6. Conclusion

Based on inductance profile variation of DSSRM, an optimum rotor shape is developed for double stator switched reluctance motor, resulting in lower torque pulsation without noticeable decrease in average torque. The proposed rotor shape is practical and easy to manufacture. Taguchi's optimization method is used for optimization Process. The optimal shape reduces the torque ripple by 69.3 % as compared with original DSSRM. The proposed rotor structure was investigated from mechanical point of view. Mechanical analysis showed that the new rotor structure is stiff against vibration and deformation. The new design makes DSSRM more suitable for Electric Hybrid Vehicles (EHVs) and other low torque ripple applications.

## Appendix A

**Table 5.** Parameters of DSSRM

| | |
|---|---|
| Number of stator poles | 8 |
| Number of rotor poles | 6 |
| Number of phases | 4 |
| Outer radius of outer stator | 72.0 mm |
| Outer radius of inner stator | 43.9 mm |
| Airgap 1 and Airgap 2 | 1.0 mm |
| Stack length | 115.0 mm |
| Number of turns per phase | 50 |
| Rated current | 20 A |
| Rated voltage | 100 V |
| Resistance per phase | 0.78 Ω |
| Lamination material | M19 |

## References

[1] M. A. Abbasian, M. Moallem, B. Fahimi, "Double Stator Switched Reluctance Machines (DSSRM): fundamentals and magnetic force analysis", IEEE Trans. on Energy Con., vol. 25, pp. 589-597, 2010.

[2] Patrick L. Chapman, Scott D. Sudhoff," Design and Precise Realization of Optimized Current Waveform for Switched Reluctance Drive" IEEE Trans. Power Electronics., vol. 17, no. 1, pp. 76-83, 2002.

[3] Mohammad S. Islam and Iqbal Husain, "Torque-Ripple Minimization with Indirect Position and Speed Sensing for Switched Reluctance Motors,"

IEEE Trans. Ind. Elec., vol. 47, no. 5, pp. 1126-1133, 2000.

[4] Iqbal Husain, M. Ehsani, "Torque Ripple Minimization in Switched Reluctance Motor Drives by PWM Current Control," IEEE Trans. Power Electronics., vol. 11, no.1, pp. 83-88, 1996.

[5] Aleksandar M. Stankovic´, Gilead Tadmor, *IEEE*, Zoran J. C´ oric´, I˙smail Agirman, "On Torque Ripple Reduction in Current-Fed Switched Reluctance Motors," IEEE Trans. Ind. Electronics., vol. 46, no. 1, pp. 177-183, 1992.

[6] M. Illic-Spong, T. J. E. Miller, S. R. MacMinn, and J. S. Thorp, "Instantaneous torque control of electric motor drives," *IEEE Trans. Power Electron.*, vol. 2, pp. 55-61, 1987.

[7] D. S. Schramm, B. W. Williams, and T. C. Green T, "Torque ripple reduction of switched reluctance motors by PWM phase current optimal profiling," in *Proc. IEEE PESC'92*, pp. 857-860, 1992.

[8] D. G. Taylor, M. J. Woolley, and M. Illic-Spong, "Design and implementation of a linearizing and decoupling feedback transformation for switched reluctance motors," in *Proc. 17th Symp. Incremental Motion Control Systems and Devices*, pp. 173-184, 1988.

[9] M. Ilic'-Spong, R. Marino, S. Peresada, and D. Taylor, "Feedback linearizing control of a switched reluctance motors," *IEEE Trans. Automat. Contr.*, vol. AC-32, pp. 371-379, 1987.

[10] Iqbal Husain, "Minimization of Torque Ripple in SRM Drives" IEEE Trans. Ind. Electronics., vol. 49, no. 1, 2002.

[11] B. Mirzaeian, M. Moallem, V. Tahani, C. Lucas, "Multiobjective Optimization Method Based on a Genetic Algorithm for Switched Reluctance Motor design," IEEE Trans. Magetics. vol. 38, pp. 1524-1527, 2002.

[12] P. C. Desai, M. Krishnamurthy, N. Schofield, A. Emadi, "Novel Switched Reluctance Machine Configuration With Higher Number of Rotor Poles Than Stator Poles: Concept to Implementation", IEEE Trans. Ind. Applicat., vol. 57, pp. 649-659, 2010.

[13] Krzysztof Russa, Iqbal Husain," Torque-Ripple Minimization in Switched Reluctance Machines Over a Wide Speed Range," IEEE Trans. Ind. Electronics., vol. 34, no. 5, pp. 1105-1112, 1998.

[14] Jin Woo Lee, Hong Seok Kim, Byung II Kown, Byung Taek Kim, "New Rotor Shape Design for Minimum Torque Ripple of SRM Using FEM," IEEE Trans. on Magnetics., vol. 40, no. 2, 2001.

[15] Yong Kwon Choi, et. al., "Pole-Shape Optimization of a Switched-Reluctance Motor for Torque Ripple Reduction," IEEE Trans. on Magnetics., vol. 43, no. 4, pp. 1797-1800, 2007.

[16] Jawad Feiz, J.W. Finch, H. M. B. Metwally, "A Novel Switched Reluctance Motor With Multiple Teeth Per Stator Pole and Comparison of Such Motors" Electric Power System Research, vol. 34, pp. 197-203, 1995

[17] Funda Sahin, H. BulentErtan, Kemal Leblebicioglu, (1995) "Optimum Geometry for Torque Ripple Minimization of Switched Reluctance Motors", COMPEL: The International Journal for Computation and Mathematics in Electrical and Electronic Engineering, vol. 14, pp 117-121.

[18] J. Corda, A. M. Tataru, P. O. Rasmussen and E. Ritchie, "Analytical Estimation of Torque Enhancement of the SR Machine with Saw-Shaped (Shark) Pole Surfaces," IEE Proc. -Electr. Power Appl., Vol. 151, No. 2, 2004.

[19] Moallem, M.; Chee-Mun Ong; Unnewehr, L., "Effect of rotor profiles on the torque of a switched-reluctance motor," Industry Applications, IEEE Transactions on, vol. 28, no. 2, pp. 364,369, 1992

[20] S. I. Nabetaet.al., "Mitigation of The Torque Ripple of a Switched Reluctance Motor Through a Multi objective optimization," IEEE Trans. Magn., vol. 44, no.6, pp. 1018-1021, June 2008.

[21] Krzysztof Russa, Iqbal Husain, Malik E. Elbuluk, "Torque-Ripple Minimization in Switched Reluctance Machines Over a Wide Speed Range," IEEE Trans. Ind. Electron., vol. 34, no. 5, pp. 1105-1112, September/October 1998.

[22] Dong-Hee Lee; Trung Hieu Pham; Jin-Woo Ahn, "Design and Operation Characteristics of Four-Two Pole High-Speed SRM for Torque Ripple Reduction," *Industrial Electronics, IEEE Transactions on*, vol. 60, no. 9, pp. 3637,3643, Sept. 2013

[23] Ghousia, Syeda Fatima S., "A Novel Globally Optimized Instantaneous Torque Ripple Minimization Method in Switched Reluctance Motors with Matrix Converter Drives" (2013). Electronic Theses and Dissertations. Paper 4913.

[24] Wei-Chung Wengr, Fan Yang, and Atef Z. Elsherbeni, "Linear Antenna Array Synthesis Using Taguchi's Method: A Novel Optimization Technique in Electromagnetics," IEEE Trans. On Antenna And Propag., vol. 55, no. 3, pp. 723-730, March 2007.

[25] J. Felba, K. P. Friedel, and A. Moscicki, "Characterization and performance of electrically conductive adhesives for microwave applications," in Proc. 4th Int. Conf. Adhesive Joining Coating Technol. Electron., Espoo, Finland, pp. 232-239, 2000.

**Mohammadali Tavakkoli** was born in Isfahan, Iran, in 1982. He received his B.S. and M.S. in electrical engineering from Amirkabir University of Technology and Isfahan University of Technology, in 2005 and 2007 respectively. His research interests are electric machine design, optimization methods and electric motor drives.

**Mehdi Moallem** received the Ph.D. degree in electrical engineering from Purdue University, West Lafayette, IN, in 1989. He is currently a Full Professor at the Department of Electrical and Computer Engineering, Isfahan University of Technology, Isfahan, Iran. He is the author or coauthor of various journal and conference papers. His research interests include design and optimization of electromagnetic devices, application of advance numerical techniques and expert systems to analysis and design of electrical machines, and power quality. Prof. Moallem was a recipient of many international and national awards.